Adaptive cell-centered finite volume method for non-homogeneous diffusion problems: Application to transport in porous media

Fayssal Benkhaldoun, Amadou Mahamane, and Mohammed Seaïd

Abstract We investigate time stepping schemes for the adaptive cell-centered finite volume solution of diffusion equations with heterogeneous diffusion coefficients. The proposed finite volume method uses the cell-centered techniques to discretize the diffusion operators on unstructured grids. Explicit and implicit time integration schemes are used and a comparative study is presented in terms of accuracy and efficiency. Numerical results are presented for a transient diffusion equation with known analytical solution. We also apply these methods to a problem of oil recovery using a two-phase flow problem in porous media.

Keywords Diffusion problems, finite volume, flow in porous media
MSC2010: 76S05, 65N08, 65Y20

1 Introduction

In the last decade, finite volume methods have offered a remarkable level of accuracy and robustness required for solving complex flow problems governed by hyperbolic systems of conservation laws. However, engineering applications often involve coupled hyperbolic and elliptic partial differential equations which have to be solved on complex geometries, thus suggesting the use of the same spatial discretization for both hyperbolic and elliptic equations. As an example of these applications where hyperbolic and elliptic equations coexist we mention

Fayssal Benkhaldoun and Amadou Mahamane
LAGA, Université Paris 13, 99 Av J.B. Clement, 93430 Villetaneuse, France,
e-mail: fayssal@math.univ-paris13.fr, mahamane@math.univ-paris13.fr

Mohammed Seaïd
School of Engineering and Computing Sciences, University of Durham, South Road,
Durham DH1 3LE, UK, e-mail: m.seaid@durham.ac.uk

J. Fořt et al. (eds.), *Finite Volumes for Complex Applications VI – Problems & Perspectives*, Springer Proceedings in Mathematics 4,
DOI 10.1007/978-3-642-20671-9_9,

the multi-phase flows in porous media, see for example [1, 3, 5]. In practice, the focus is on unstructured meshes where a non-trivial reconstruction scheme is required to have a high-order spatial accuracy. Most of upwind finite volume methods for unstructured grids proposed to date employ a cell-vertex discretization, since it allows a natural definition of the flow gradients: using a dual mesh, a gradient-based reconstruction is applied on the two sides of each interface, where an approximate Riemann solver is finally applied to select the proper upwind contributions. However, solving diffusion equations using the finite volume methods is still a considerable task in the case of unstructured meshes; particularly when these equations have to be solved in conjunction with partial differential equations of hyperbolic type. The emphasis in this work is on the time integration of the resultant system of ordinary differential equations induced from cell-centered finite volume discretization in space variable of the transient diffusion problems. The proposed schemes are the explicit Euler and implicit Euler scheme. These two different methods lead to techniques all of which are occurring in time integration framework since years. Theoretical considerations can provide some ideas concerning stability, convergence rates, restriction on time stepsizes, or qualitative behaviour of the solution, but a complete quantitative analysis is not possible today. Therefore, the only way to make a judgment is to perform numerical tests, at least for some problems which seem to be representative. However, looking into the literature, it seems that there have not been many studies of this type which can give satisfactory answers.

2 Adaptive cell-centered finite volume method

Our main concern in the present study is on the finite volume discretization of the two-dimensional gradient operator $\nabla = \left(\frac{\partial}{\partial x}, \frac{\partial}{\partial y}\right)^T$ resulting from the weak formulation of the diffusion equations. To this end we discretize the spatial domain $\bar{\Omega} = \Omega \cup \partial\Omega$ in conforming triangular elements K_i as $\bar{\Omega} = \cup_{i=1}^{N} K_i$, with N is the total number of elements. Each triangle represents a control volume and the variables are located at the geometric centers of the cells. To discretize the diffusion operators we adapt the so-called cell-centered finite volume method based on a Green-Gauss diamond reconstruction, see for example [5] and further references are therein. Hence, a co-volume, D_σ, is first constructed by connecting the barycentres of the elements that share the edge σ and its endpoints as shown in Fig. 1. Then, the discrete gradient operator ∇_σ is evaluated at an inner edge σ as

$$\nabla_\sigma u_h = \frac{1}{2\text{meas}(D_\sigma)}\big((u_L - u_K)\text{meas}(\sigma)\mathbf{n}_{K,\sigma} + (u_S - u_N)\text{meas}(s_\sigma)\mathbf{n}'_\sigma\big), \qquad (1)$$

where u_h is the finite volume discretization of a generic function u, meas(D) denotes the area of the element D, $\mathbf{n}_{K,\sigma}$ denotes the unit outward normal to the surface σ, u_K and u_L are the values of the solution u_h in the elements K and L, respectively. In (1),

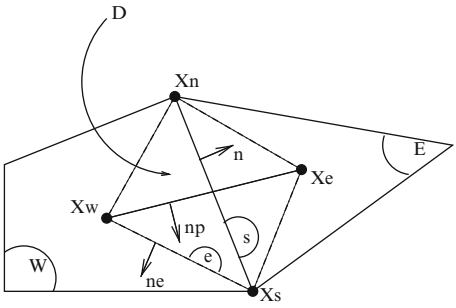

Fig. 1 A generic two-dimensional finite volume and notations

u_S and u_N are the values of the solution u_h at the co-volume nodes approximated by a linear interpolation from the values on the cells sharing the same vertex S and N, respectively. For further details on the formulation and analysis of the considered cell-centered finite volume method we refer to [4, 5] among others.

The treatment of boundary conditions in the cell-centered finite volume method is performed using similar techniques as those described in [2, 5]. In order to improve the efficiency of the proposed finite volume method, we have performed a mesh adaptation to construct a nearly optimal mesh able to capture the small solution features without relying on extremely fine grid in smooth regions far from steep gradients. In the present work, this goal is achieved by using an error indicator for the gradient of the solution. This indicator requires only information from solution values within a single element at a time and it is easily calculated, see for instance [2].

3 Time stepping schemes

For simplicity in the presentation we consider the transient diffusion problem

$$\frac{\partial u}{\partial t} - \nabla \cdot (\mathbb{K}(\mathbf{x})\nabla u) = f(\mathbf{x}, t), \qquad (\mathbf{x}, t) \in \Omega \times (0, T], \tag{2}$$

where Ω is a subset of $\mathbb{R}^2$ with smooth boundary $\partial\Omega$, $(0, T]$ is the time interval, $\mathbb{K}(\mathbf{x})$ is a 2×2 matrix with entries k_{ij}, and $f(\mathbf{x}, t)$ is an external force. In the current study the spatial discretization of the diffusion equation (2) is carried out using the cell-centered finite volume method and two time stepping schemes are considered for the time integration.

For the time integration of (2) we discretize the time interval into subintervals $[t_n, t_{n+1}]$ with length Δt, $0 = t_0, t_1, \ldots, t_N = T$ and $t_n = n\Delta t$. We use the notation ω^n to denote the value of a generic function ω at time t_n. Hence, using the forward Euler method, the fully discrete version of the diffusion equation (2) reads

$$u_K^{n+1} = u_K^n + \frac{\Delta t}{\text{meas}(K)} \sum_{\sigma \in \mathscr{E}_K} F_{K,\sigma}\left(u_h^n\right) \text{meas}(\sigma) + \Delta t f_K^n, \qquad \forall\ K \in \mathscr{T}, \quad (3)$$

where $\mathscr{E}_K$ is the set of all edges of the control volume K and $F_{K,\sigma}^n$ are the numerical fluxes reconstructed as

$$F_{K,\sigma}(u) = \mathbb{K}_\sigma \nabla_\sigma u \cdot \mathbf{n}_{K,\sigma}, \quad (4)$$

with $\mathbb{K}_\sigma$ is an averaged values of the diffusion matrix $\mathbb{K}$ on the edge σ and ∇_σ is the cell-centered finite volume discretization of the gradient operator defined in (1).

An implicit time stepping scheme for (2) is formulated using the backward Euler scheme as

$$u_K^{n+1} = u_K^n + \frac{\Delta t}{\text{meas}(K)} \sum_{\sigma \in \mathscr{E}_K} F_{K,\sigma}\left(u_h^{n+1}\right) \text{meas}(\sigma) + \Delta t f_K^{n+1}, \qquad \forall\ K \in \mathscr{T}. \quad (5)$$

To find the solution u_K^{n+1} from (5) one has to solve, at each time level, a linear system of algebraic equations. In our simulations, the linear system is solved using the preconditioned GMRES solver with a convergence criteria of 10^{-6}, we use the diagonal as a preconditionner.

4 Numerical Results

In this section we examine the accuracy and performance of the proposed time stepping schemes using two test examples. The first example solves a transient diffusion equation with analytical solution that can be used to quantify errors in the time stepping schemes. The second example considers a problem of oil recovery using the equations of two-phase flows in porous media. This last example is used to qualify the considered implicit time stepping scheme for more complicated nonlinear convection-dominated flows. In all the computations reported herein, a two-level refining and fixed CFL numbers are used.

4.1 Accuracy test problem

First we consider the problem of a diffusion problem with manufactured exact solution in a squared domain $\Omega = [-1, 1] \times [-1, 1]$. Here, we solve the transient equation (2) subject to a nonhomogenuous diffusion tensor given by

$$\mathbb{K} = (1 + \alpha x)^2 \begin{pmatrix} 1 & 10^{-2} \\ 10^{-2} & 10^{-6} \end{pmatrix}. \quad (6)$$

The reaction term f is explicitly calculated such that the exact solution of the diffusion problem (2) and (6) is

$$U(x, y, t) = \sin(\pi x)\sin(\pi y)\left(1 - \mathrm{e}^{-\lambda t}\right). \tag{7}$$

In our computations $\alpha = \lambda = 0.1$, the initial condition is calculated from the analytical solution (7) and homogeneous Dirichlet boundary conditions are imposed on $\partial\Omega$. To quantify the errors in this test example we consider the L^2-error norm defined as

$$\|e_h\| = \left(\sum_{K\in\mathscr{T}} \mathrm{meas(K)e_K^2}\right)^{\frac{1}{2}},$$

where $e_K(T) = |U_K - u_K|$ with u_K and U_K are respectively, the computed and exact solutions on the control volume K. In the current study, we present numerical results at the transient regime corresponding to the simulation time $T = 1$.

Table 1 Relative error and statistics using the explicit and implicit schemes at the transient time $T = 1$ and different CFL numbers. min Δt is the minimum Δt used in the scheme and GMRES iter refers to the mean number of iterations in the GMRES solver

	Explicit scheme	Implicit scheme			
	CFL = 1	CFL = 5	CFL = 10	CFL = 50	CFL = 100
Coarse mesh					
min Δt	4.70E-04	2.35E-03	4.70E-03	2.35E-02	4.70E-02
Relative error	1.15E-02	9.65E-03	8.07E-03	1.44E-02	3.49E-02
# time steps	2126	426	213	43	22
CPU time	0.76	0.44	0.32	0.20	0.16
GMRES iter	—	5	8	28	44
# elements	896	896	896	896	896
# nodes	481	481	481	481	481
Fine mesh					
min Δt	7.32E-06	3.66E-05	7.32E-05	3.66E-04	7.32E-04
Relative error	1.73E-04	1.41E-004	1.097E-04	1.958E-04	5.569E-04
# time steps	136576	27316	13658	2732	1366
CPU time	4814.781	2187.42	1415.296	1981.735	1297.94
GMRES iter	—	2	4	29	42
# elements	57344	57344	57344	57344	57344
# nodes	28929	28929	28929	28929	28929
Adaptive mesh					
min Δt	8.91E-06	4.46E-05	8.92E-05	4.46E-04	8.91E-04
Relative error	1.83E-03	1.82E-03	1.80E-03	1.918E-03	2.12E-03
# time steps	112120	22383	11166	2192	1070
CPU time	1496.57	595.63	294.846	148.28	124.38
GMRES iter	—	2	3	9	19
# elements	17256	17249	17248	16480	15507
# nodes	8681	8676	8676	8292	7806

To quantify the considered time stepping schemes applied to this example we summarize in Table 1 the results obtained at the transient time $T = 1$. In this table we present the minimum time stepsize, the relative error, the number of time steps required to reach the steady state, the CPU time in seconds, the number of iterations in the GMRES solver, the number of elements and the number of nodes in the considered meshes. A simple inspection of these results shows that

the implicit schemes can use larger CFL numbers than those required for a stable explicit scheme. Note that using large CFL numbers in the implicit scheme results in a decrease on the number of time steps needed to reach the steady state and at the same time results in an increase on the number of the iterations in the GMRES solver. As expected the highest accuracy is obtained for both explicit and implicit schemes on the fine mesh but with a large CPU time compared to the results on coarse and adaptive meshes. No remarkable difference is obtained in the relative errors for the implicit and explicit schemes on the coarse and fine meshes. However, using an adaptive mesh the implicit scheme produces smaller errors than the explicit scheme. On the other hand, due to grid adaptation the final mesh at CFL = 100 consists of 15507 cells only compared to the 57344 cells for the fixed fine mesh. This results in a significant reduction of the computational cost. An examination of the CPU times in the tables reveals that, the cell-centered finite volume method on fixed meshes requires more computational work than its adaptive counterpart.

4.2 Transport in porous media

We solve a problem of oil recovery in a two-dimensional porous reservoir. The problem statement is solving a two-phase flow problem in porous media on the computational domain defined by $\bar{\Omega} = \Omega \cup \partial\Omega$ with $\partial\Omega = \Gamma_1 \cup \Gamma_2 \cup \Gamma_3$ as illustrated in Fig. 2. Here, the governing equations consist of the pressure equation

$$\begin{aligned} \mathbf{q} &= -d(u)\mathbb{K}(\mathbf{x})\nabla p, && (\mathbf{x},t) \in \Omega \times (0,T], \\ \nabla \cdot \mathbf{q} &= 0, && (\mathbf{x},t) \in \Omega \times (0,T], \\ \mathbf{q}\cdot\mathbf{n}\big|_{\Gamma_1} &= -1.4, \quad \mathbf{q}\cdot\mathbf{n}\big|_{\Gamma_2} = 0, \quad p\big|_{\Gamma_3} = 0, && t \in (0,T], \end{aligned} \tag{8}$$

and the saturation equation

$$\begin{aligned} \phi(\mathbf{x})\frac{\partial u}{\partial t} - \nabla\cdot\big(b(u)\mathbf{q} - \mathbb{K}(\mathbf{x})a(\mathbf{x})\nabla u\big) &= 0, && (\mathbf{x},t) \in \Omega \times (0,T], \\ u\big|_{\Gamma_1} = 1, \quad \mathbb{K}\cdot\mathbf{n}\big|_{\Gamma_2} = 0, \quad u\big|_{\Gamma_3} &= 0, && t \in (0,T], \\ u(\mathbf{x},0) &= u_0(\mathbf{x}), && \mathbf{x} \in \Omega, \end{aligned} \tag{9}$$

where p is the pressure, $\mathbf{q}$ the Darcy velocity, u the saturation, $\mathbb{K}$ is the permeability of the medium, ϕ the porosity and $d(u) = k_w(u) + k_o(u)$ is the total mobility with $k_w(u)$ and $k_o(u)$ are the mobility of water and oil, respectively. In (9),

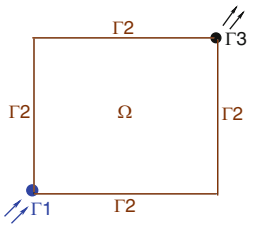

Fig. 2 Computational domain for the example of transport in porous media

$$b(u) = \frac{k_w(u)}{k_w(u) + k_o(u)}, \qquad a(u) = \frac{k_w(u)k_o(u)}{k_w(u) + k_o(u)} p'(u),$$

with $p(u)$ represents the capillary pressure. Note that, in most practical applications, the effects of Darcy velocity dominates the effects of diffusion. As a consequence the saturation equation (9) results in a convection-dominated problem which requires special numerical treatment and many numerical methods from the literature fail to accurately approximate its solution. In addition, since the diffusion in (9) depends on the Darcy velocity, the accuracy on the solution of saturation equation (9) strongly needs an accurate solution of the pressure equation (8). For more details on this model we refer the reader to [1, 3, 5] among others. In our simulations, the permeability $\mathbb{K} = Id$, with Id is the 2×2 identity matrix, the porosity $\phi = 0.2$, the water and oil mobility along with the capillary pressure are given by

$$k_w(u) = \frac{1}{2}u^5, \qquad k_o(u) = \frac{1}{3}(1-u)^3, \qquad p(u) = -\sqrt{\frac{1-u}{u}}.$$

The initial condition u_0 is defined as

$$u_0(\mathbf{x}) = \begin{cases} 1, & \text{if} \quad \mathbf{x} \in \Gamma_1, \\ 0, & \text{elsewhere.} \end{cases}$$

This problem has an interesting structure and will be used to verify the adaptive cell-centered finite volume method namely, to verify that the adaptation methodology is able to compute the right speed of the saturation fronts, and to verify that adaptive refinement is computationally cheaper than fixed mesh for a given level of solution resolution. Based on the conclusions drawn in the previous test example, only results using the implicit time stepping scheme are presented for this example. Figure 3 shows the adapted meshes and plots of the saturation at two different times, namely $t = 0.022$ and $t = 0.048$. The initial mesh contains 3662 cells and a $\Delta t = 2 \times 10^{-5}$ is used in our simulations. At earlier time of the simulation, the front entering the reservoir starts to develop and will be advected later on by the flow at far exit

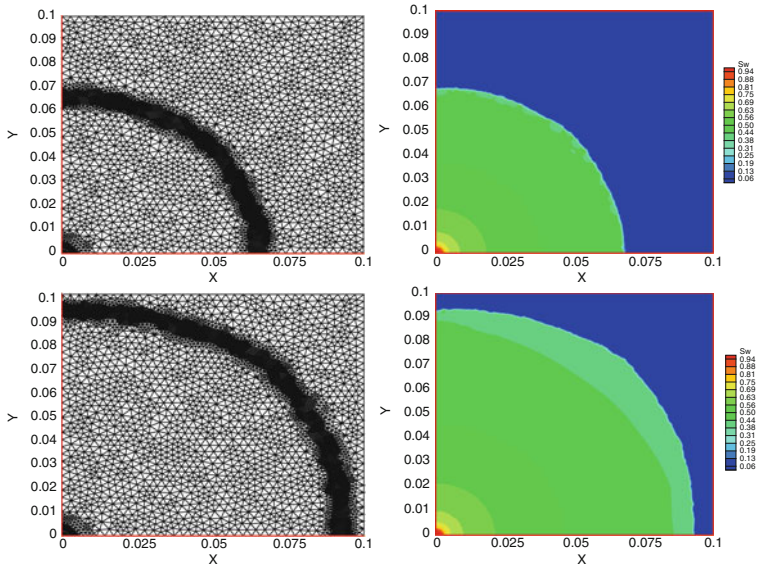

Fig. 3 Adaptive meshes and saturation contours at time $t = 0.022$ (top) and $t = 0.048$ (bottom)

of the reservoir. The interaction between the Darcy pressure and the saturation is detected across the reservoir during the simulation time. It can be clearly seen that the saturation front structures being captured by the cell-centered finite volume method. Another important result is that positions of the saturated waves are not deteriorated by the multiple mesh adaptations. The adaptive cell-centered finite volume method accurately approximates the solution to this problem of two-phase flow in porous media. In addition, the comparison with similar numerical results available in the literature [1] on the same test case is also satisfactory. It should be stressed that, due to grid adaptation the final mesh at times $t = 0.022$ and $t = 0.048$ consists of 4039 and 4947 cells, respectively. This results in a significant reduction of the computational cost compared to a cell-centered finite volume method on fixed meshes.

References

1. M. Afif, B. Amaziane, Convergence of finite volume schemes for degenerate convection-diffusion equation arising in flow in porous media, *Comput. Methods Appl. Mech. Engrg.* (2002) 5265–5286.
2. F. Benkhaldoun, I. Elmahi and M. Seaïd, Well-balanced finite volume schemes for pollutant transport by shallow water equations on unstructured meshes, *J. Comput. Phys.* **226** (2007) 180–203.
3. G. Chavent, J. Jaffré, *Mathematical models and finite element for reservoir simulation*, North-Holland. 1986.

4. Y. Coudière, J.P. Vila, P. Villedieu, Convergence rate of finite volume scheme for a two dimensional convection-diffusion problem, *M2AN*. **33** (1999) 493–516.
5. A. Mahamane, Analyse et estimation d'erreur en volumes finis, Application aux écoulements en milieu poreux et á l'adaptation de maillage, *Dissertation, Université Paris 13*, 2009.

The paper is in final form and no similar paper has been or is being submitted elsewhere.